

# Engineering of nonclassical motional states in optomechanical systems

Xun-Wei Xu,<sup>1</sup> Hui Wang,<sup>1</sup> Jing Zhang,<sup>2,3</sup> and Yu-xi Liu<sup>1,3,\*</sup>

<sup>1</sup>*Institute of Microelectronics, Tsinghua University, Beijing 100084, China*

<sup>2</sup>*Department of Automation, Tsinghua University, Beijing 100084, P. R. China*

<sup>3</sup>*Tsinghua National Laboratory for Information Science and Technology (TNList), Tsinghua University, Beijing 100084, China*

(Dated: January 22, 2018)

We propose to synthesize arbitrary nonclassical motional states in optomechanical systems by using sideband excitations and photon blockade. We first demonstrate that the Hamiltonian of the optomechanical systems can be reduced, in the strong single-photon optomechanical coupling regime when the photon blockade occurs, to one describing the interaction between a driven two-level trapped ion and the vibrating modes, and then show a method to generate target states by using a series of classical pulses with desired frequencies, phases, and durations. We further analyze the effect of the photon leakage, due to small anharmonicity, on the fidelity of the expected motional state, and study environment induced decoherence. Moreover, we also discuss the experimental feasibility and provide operational parameters using the possible experimental data.

PACS numbers: 42.50.Dv, 42.50.Wk, 07.10.Cm

## I. INTRODUCTION

Whether macroscopic mechanical resonators behave quantum mechanics is a long-outstanding debate of the fundamental physics [1–3]. Recent experimental progresses on, e.g., ground-state cooling and the fabrication of high-frequency mechanical resonators, push forward the process to end this debate. In existing literatures, several methods have been proposed to cool the mechanical resonators to their ground state in various types of the nano-structures, e.g., doubly clamped beams, singly clamped cantilevers, radial breathing modes of micro-toroids, and membranes. The potential applications of mechanical resonators in the quantum regime can be referred to, e.g., quantum information processing and sensitive quantum detection of very weak forces.

It is well known that quantum superpositions are main resources for quantum information processing. Many theoretical proposals and experimental demonstrations have been presented to generate and manipulate quantum superposed states. For example, we have theoretically studied how to generate superpositions of different Fock states for microwave photons [4], and later on experimentalists produced Fock states [5] and arbitrary superpositions [6] of different Fock states by coupling a single-mode microwave cavity field to a superconducting phase qubit. Similarly, particular nonclassical phonon states of the vibrational mode of trapped ions have been theoretically studied [7–10] and experimentally demonstrated [11, 12]. However, the generation of arbitrary nonclassical motional states (hereafter, we call them as phonon states) in macroscopic mechanical resonators with low-frequencies is still an open question.

Macroscopic mechanical resonators in the quantum regime can be manipulated by integrating them with other quantum components. For instance, the superpositions of macroscopically distinct quantum states have been theoretically studied in a mechanical resonator by coupling it to a charge qubit [13].

The quantum ground state and single-phonon control [14] have been experimentally demonstrated for a microwave-frequency mechanical resonator coupled to a phase qubit. This circuit-QED-like system [14] makes it possible to engineer arbitrary phonon states in a deterministic way as for microwave photon states [4–6]. The recent studies demonstrate that optomechanical systems [2, 3] can provide another platform to control and manipulate the quantum states of the low-frequency mechanical resonator by coupling it to a cavity field. In particular, experiments [15–18] showed that the optomechanical systems are approaching the strong single-photon coupling regime.

It has been shown that the photon blockade can occur [19–24] in the strong single-photon optomechanical coupling when single-photons pass through the cavity of the optomechanical system. We here study a method to synthesize arbitrary nonclassical phonon states in optomechanical systems by using photon blockade and a series of sideband excitations with desired durations. We mention that the red sideband excitations were studied theoretically [25, 26] and experimentally [27–32] for the ground state cooling of the mechanical resonators. In contrast to the method of the measurement-based [33–35] non-Gaussian phonon state generation [36, 37] in optomechanical systems, our method is deterministic one as for microwave single-phonon generation [14]. But here we need sideband excitations to make the low frequency mechanical resonator to resonantly interact with the high frequency cavity field, assisted by the driving field with the frequency matching condition, the microwave single-phonon generation requires no sideband excitations [14].

The purpose of this paper is to present a method on the preparation of the arbitrary nonclassical phonon states in optomechanical systems. We will mainly analyze detailed steps, possible errors and experimental feasibilities. In Sec. II, the theoretical model of the optomechanical system is introduced, an effective Hamiltonian is derived in the strong single-photon optomechanical coupling regime. We find that this effective Hamiltonian is equivalent to one of trapped ions [38]. In Sec. III, we show how to synthesize phonon states by using sideband excitation and the effective Hamiltonian derived in

---

\*Electronic address: yuxiliu@mail.tsinghua.edu.cn

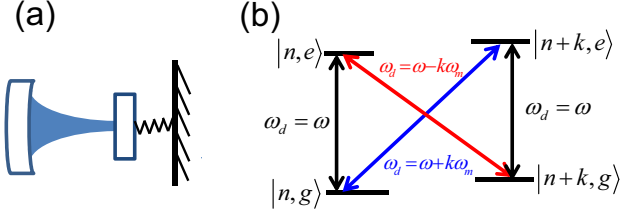


FIG. 1: (Color online) (a) Schematic diagram for optomechanical systems with the radiation-pressure type interaction: the cavity can be in either the optical, or the microwave, or the radio-wave regime; and the mechanical resonator can be doubly clamped beams, singly clamped cantilevers, radial breathing modes of micro-toroids, and membranes. (b) Three different transition processes are presented by the black (carrier), red ( $k$ -phonon red sideband excitation) and blue ( $k$ -phonon blue sideband excitation) arrow lines.

Sec. II. In Sec. IV, we analyze the effect of the photon leakage on the fidelity of the expected target state due to small anharmonicity. In Sec. V, the environmental effect on prepared states is further studied. Moreover, we discuss the experimental feasibility and provide operational parameters in Sec. VI. The conclusions are finally given in Sec. VII.

## II. THEORETICAL MODEL

We study an optomechanical system, which can be the membrane coupled to an optical cavity, or the optical cavity with one-end movable mirror, or the superconducting transmission line resonator coupled to a mechanical beam. As schematically shown in Fig. 1(a), such system has the radiation-pressure-type interaction, and the Hamiltonian of the system driven by a classical field can be written as

$$H = \hbar\omega_c a^\dagger a + \hbar\omega_m b^\dagger b + \hbar g a^\dagger a (b^\dagger + b) + \hbar\Omega \left[ a^\dagger e^{-i(\omega_d t + \phi_d)} + \text{h.c.} \right]. \quad (1)$$

Here,  $a^\dagger$  ( $a$ ) is the creation (annihilation) operator of the cavity field with the frequency  $\omega_c$ , and  $b^\dagger$  ( $b$ ) is the creation (annihilation) operator of the mechanical resonator with the frequency  $\omega_m$ . The parameter  $g$  describes the coupling strength between the cavity field and the mechanical resonator. The parameter  $\Omega$  is the coupling strength between the cavity field and the external driving field with the frequency  $\omega_d$  and the phase  $\phi_d$ .

If an unitary transform  $U = \exp[ga^\dagger a (b^\dagger - b)/\omega_m]$  is applied to Eq. (1), then the Hamiltonian in Eq. (1) becomes

$$H_{\text{eff}} = \hbar\omega a^\dagger a - \hbar \frac{g^2}{\omega_m} a^\dagger a^\dagger a a + \hbar\omega_m b^\dagger b + \hbar\Omega \left\{ a^\dagger e^{[\eta(b^\dagger - b) - i(\omega_d t + \phi_d)]} + \text{h.c.} \right\}, \quad (2)$$

where  $\omega = \omega_c - g^2/\omega_m$  and  $\eta = g/\omega_m$ . It is obvious that the energy structure of the photon Hamiltonian, corresponding to the first two terms in the right hand of Eq. (2), becomes

anharmonic one due to the photon-photon interaction induced by the radiation pressure. Moreover, the nonlinear photon-photon interaction term  $\hbar g^2 a^{\dagger 2} a^2 / \omega_m$  guarantees the photon blockade [20] in the optomechanical systems with the strong coupling strength  $g$  and low dissipation of the cavity field, i.e.,  $(g^2/\omega_m) > \gamma_c$  with the decay rate  $\gamma_c$  of the cavity field. In this case, the driving field couples only two lowest energy levels  $|0\rangle$  and  $|1\rangle$  of the cavity field, and Eq. (2) can be further reduced to

$$H_{\text{tw}} = \hbar \frac{\omega}{2} \sigma_z + \hbar\omega_m b^\dagger b + \hbar \left\{ \Omega(t) \sigma_+ e^{\eta(b^\dagger - b)} + \text{h.c.} \right\}, \quad (3)$$

under the two-level approximation for the cavity field with

$$\Omega(t) = \Omega \exp[-i(\omega_d t + \phi_d)].$$

Here, we redefine the photon operators  $a^\dagger$  and  $a$  via the ladder operator  $\sigma_+ = |1\rangle\langle 0|$  and  $\sigma_- = |0\rangle\langle 1|$  in the basis of two states  $|0\rangle$  and  $|1\rangle$  of the cavity field. We also define the Pauli operator  $\sigma_z = |1\rangle\langle 1| - |0\rangle\langle 0|$ . Hereafter, we use  $|e\rangle$  and  $|g\rangle$  to denote the single-photon excited state  $|1\rangle$  and the vacuum (ground) state  $|0\rangle$  of the cavity field, respectively, i.e.,  $|1\rangle \equiv |e\rangle$  and  $|0\rangle \equiv |g\rangle$ . Moreover, the states  $|k\rangle$  with  $k = 1, 2, \dots, N$  denote the phonon number states of the mechanical resonator with the transform  $U$ .

The effective Hamiltonian in Eq. (3) is similar to one that describes the interaction between a classical driving field and a single two-level trapped cold ion vibrating along one-direction [38]. That is, the two-level trapped cold ion, the vibrating mode of the trapped ion and the classical driving field are equivalent to the two-level system constructed by two lowest energy levels of the cavity field, the vibrating mode of the mechanical resonator, the classical field applied to the cavity, respectively. The parameter  $\eta$  is equivalent to the Lamb-Dicke parameter in the system of trapped ion. The third term in Eq. (3) can be further written as

$$H_{\text{th}} = \hbar\Omega(t) e^{-\frac{\eta^2}{2}} \sigma_+ \sum_{j,l} \frac{(-1)^l \eta^{(j+l)} b^{\dagger j} b^l}{j! l!} + \text{h.c.}, \quad (4)$$

which can be reduced to the carrier, or red sideband excitation or blue sideband excitation process in different resonant conditions with the language of trap ions [38].

As schematically shown in Fig. 1, the  $k$ -phonon red sideband excitation process links the transitions between  $|n, e\rangle$  and  $|n+k, g\rangle$  under the condition  $\omega_d = \omega - k\omega_m$ , with an effective Rabi frequency

$$\Omega_{n,k} = \Omega e^{(-\eta^2/2)} \eta^k \sqrt{\frac{(n+k)!}{n!}} \sum_{j=0}^n \frac{(-1)^j \eta^{2j} C_n^j}{(j+k)!} \quad (5)$$

here  $C_n^j = n!/[j!(n-j)!]$ , i.e., the cavity field transits from the ground (excited) state to the excited (ground) state by absorbing (emitting)  $k$  phonons assisted by the external field. The  $k$ -phonon blue sideband excitation links transition between  $|n, g\rangle$  and  $|n+k, e\rangle$  under the condition  $\omega_d = \omega + k\omega_m$ , with an effective Rabi frequency  $\Omega_{n,k}$  as shown in Eq. (5), i.e., the cavity field transits from the ground (excited) state to

the excited (ground) state by emitting (absorbing)  $k$  phonons with the help of the external field. The carrier process links the transitions between  $|n, e\rangle$  and  $|n, g\rangle$  under the condition  $\omega_d = \omega$ , with an effective Rabi frequency  $\Omega_{n,0}$  given by Eq. (5) with  $k = 0$ . Therefore, no phonon absorption or emission occurs and the external field only flips the photon states in the carrier process. Under the condition (Lamb-Dicke limit)

$$\eta\sqrt{\bar{n}+1} = \frac{g}{\omega_m}\sqrt{\bar{n}+1} \ll 1 \quad (6)$$

with the average phonon number  $\bar{n}$  of the mechanical vibration, we have

$$\exp[\eta(b^\dagger - b)] \approx 1 + \eta(b^\dagger - b). \quad (7)$$

In this case, only a single-phonon transition occurs with the help of the driving field for  $k = 1$  in Fig. 1(b). The time evolution operators for the carrier, red and blue sideband processes, described by  $U_0^c(t^c)$ ,  $U_{n,k}^r(t^r)$ , and  $U_{n,k}^b(t^b)$ , are given in Appendix A, here the superscripts denote different processes, e.g.,  $r$  denotes the red sideband excitation process.

### III. SYNTHESIZING PHONON STATES

We have reduced the Hamiltonian in Eq. (1) of the driven optomechanical system to Eq. (4), which is similar to that of trapped ions [38]. Thus, arbitrary superpositions of different phonon number states  $|k\rangle$

$$|\psi\rangle = \sum_{k=0}^N c_k |k\rangle, \quad \sum_{k=0}^N |c_k|^2 = 1. \quad (8)$$

can be generated by using similar method as in the system of the trap ions [7–9], where  $|c_k|^2$  is the probability corresponding to the phonon number state  $|k\rangle$ . We clarify Eq. (8) denotes the phonon state without the transform  $U = \exp[ga^\dagger a(b^\dagger - b)/\omega_m]$ . In the following, our study on state preparation is in the basis with the transform  $U$ . However, the target state of the whole system is  $|\psi\rangle|g\rangle$ , which is not changed with an inversion of the transform  $U$  because  $U^\dagger|g\rangle = U|g\rangle = |g\rangle$ .

Under the condition  $\eta \ll 1$ , we only consider single-phonon transitions assisted by the driving field. In this case, the arbitrary phonon state as in Eq. (8) can be prepared by using the method given in Ref. [7]. We need  $N$ -step red sideband excitations and  $N$ -step carrier processes for such state preparation. The whole process can be described as

$$U_T(t)|0, g\rangle = \sum_{k=0}^N c_k |k, g\rangle \equiv \left[ \sum_{k=0}^N c_k |k\rangle \right] |g\rangle, \quad (9)$$

with a total time evolution operator  $U_T(t)$ , decomposed as

$$U_T(t) = U_1^r(t_{2N}^r) U^c(t_{2N-1}^c) \cdots U_1^r(t_{2(i+1)}^r) U^c(t_{2i+1}^c) \cdots U_1^r(t_2^r) U^c(t_1^c), \quad (10)$$

and total time

$$t = \sum_{i=1}^N (t_{2i}^r + t_{2i-1}^c), \quad (11)$$

here the superscript “ $r$ ” and “ $c$ ” denote the red-side excitation and carrier process, respectively. The time intervals and phases in each process can be calculated by following the method given in Refs. [7, 39, 40]. The main steps are to find  $U^\dagger(t)$  such that

$$|0, g\rangle = U^\dagger(t) \sum_{k=0}^N c_k |k, g\rangle. \quad (12)$$

In each step, the conditions

$$\langle i, g | U_1^{r\dagger}(t_{2i}^r) |\Psi_i\rangle = 0, \quad (13)$$

$$\langle i-1, e | U^{c\dagger}(t_{2i-1}^c) U_1^{r\dagger}(t_{2i}^r) |\Psi_i\rangle = 0, \quad (14)$$

should be satisfied. Where

$$|\Psi_i\rangle = U^{c\dagger}(t_{2i+1}^c) U_1^{r\dagger}(t_{2(i+1)}^r) \cdots U^{c\dagger}(t_{2N-1}^c) U_1^{r\dagger}(t_{2N}^r) \sum_{k=0}^N c_k |k, g\rangle. \quad (15)$$

The conditions (13) and (14) provide the equations to determine the time intervals and phases in each process as follow:

$$\tan(\Omega_{i,1} t_{2i}^r) = \frac{-i\beta_i e^{-i\phi_r^{2i}}}{\alpha_i}, \quad (16)$$

$$\tan(\Omega_{i-1,0} t_{2i-1}^c) = \frac{i\nu_i e^{i\phi_c^{2i-1}}}{\mu_i} \quad (17)$$

where

$$\alpha_i = \langle i-1, e | \Psi_i \rangle, \quad (18)$$

$$\beta_i = \langle i, g | \Psi_i \rangle, \quad (19)$$

$$\mu_i = \langle i-1, g | U_1^{r\dagger}(t_{2i}^r) |\Psi_i \rangle, \quad (20)$$

$$\nu_i = \langle i-1, e | U_1^{r\dagger}(t_{2i}^r) |\Psi_i \rangle. \quad (21)$$

Therefore, using Eqs. (16-21), we can obtain all time intervals and phases, and thus the expected state can be prepared.

Out of the regime  $\eta \ll 1$ , the arbitrary phonon state in Eq. (8) can be prepared by sequentially applying  $N$  red-sideband excitations after a carrier process as shown in Ref. [9]. That is, the cavity field is first driven by the classical field with the frequency matching condition  $\omega_d = \omega$ , then with a time interval  $t_0^c$ , the system evolves to

$$|0, g\rangle \xrightarrow{U_{0,0}^c(t_0^c)} c_0 |0, g\rangle - i e^{-i\phi_c^0} \sin(\Omega_{0,0} t_0^c) |0, e\rangle \quad (22)$$

according to the evolution operator  $U_{0,0}^c(t_0^c)$  of the carrier process in Eq. (A8) of the Appendix A, here  $c_0 = \cos(\Omega_{0,0} t_0^c)$ . After the carrier process,  $N$  red-sideband excitations are sequentially applied to the cavity with the frequency matching

conditions  $\omega_d = \omega - \omega_m, \omega - 2\omega_m, \dots, \omega - N\omega_m$  for the time intervals  $t_1^r, \dots, t_N^r$ , respectively. Then the system will evolve according to the evolution operators in Eq. (A5) of the Appendix A and the target state can be obtained. For example, in the first red-sideband excitation with the evolution operator  $U_{0,1}^r(t_1^r)$ , if the phase and the time interval are chosen such that

$$c_1 = e^{i(\phi_r^1 - \phi_c^0)} \sin(\Omega_{0,0}t_0^c) \sin(\Omega_{0,1}t_1^r), \quad (23)$$

then state of the system evolves to

$$|\Psi\rangle = c_0 |0, g\rangle + c_1 |1, g\rangle - ie^{-i\phi_c^0} \sin(\Omega_{0,0}t_0^c) \cos(\Omega_{0,1}t_1^r) |0, e\rangle. \quad (24)$$

after the first red sideband excitation. We can properly chose the the phase  $\phi_r^k$  and duration  $t_k^r$  of the  $N$  red sideband excitations such that

$$c_k = \begin{cases} \cos(\Omega_{0,0}t_0^c) & k = 0, \\ (-1)^{k-1} e^{i(\phi_r^k - \phi_c^0)} \sin(\Omega_{0,0}t_0^c) \prod_{j=1}^{k-1} \cos(\Omega_{0,j}t_j^r) \sin(\Omega_{0,k}t_k^r) & 1 \leq k \leq N-1, \\ (-1)^{N-1} e^{i(\phi_r^N - \phi_c^0)} \sin(\Omega_{0,0}t_0^c) \prod_{j=1}^{N-1} \cos(\Omega_{0,j}t_j^r) & k = N, \end{cases} \quad (25)$$

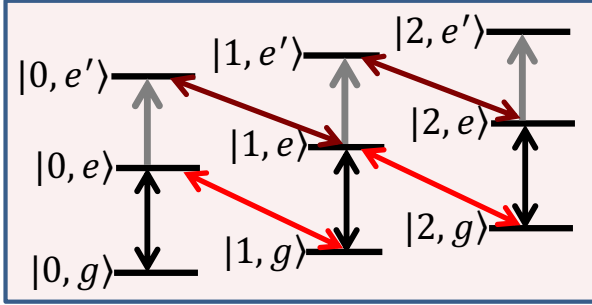


FIG. 2: (Color online) Schematic diagram for the information leakage to the third level due to the small anharmonicity. Here, two lowest horizontal lines in each column linked by the vertical black line with two arrows denote two-level approximation with the carrier process. The gray vertical line with the arrow pointed to the top line in each column simply denotes the information leakage in the carrier process. However, each red (dark red) slanted line with two arrows pointed to two black lines in different columns denotes the red sideband excitation (information leakage in the red sideband excitation). The first and second letter in the states, e.g.  $|g, 0\rangle$ , denote that the cavity field and the mechanical resonator are the ground state  $|g\rangle$  and the vacuum state  $|0\rangle$ , respectively.

then we can obtain

$$|\Psi\rangle = \sum_{k=0}^N c_k |k, g\rangle \equiv \sum_{k=0}^N c_k |k\rangle \otimes |g\rangle, \quad (26)$$

which is a product state of the target phonon state in Eq. (8) and the ground state  $|g\rangle$  of the cavity field.

#### IV. INFORMATION LEAKAGE DUE TO SMALL ANHARMONICITY

In the above, our discussions for generating an arbitrary phonon state are based on the two-level approximation of the cavity field. That is, the photon states is confined to the two-dimensional Hilbert space in the basis of photon states  $|g\rangle$  and  $|e\rangle$  (or  $|0\rangle$  and  $|1\rangle$ ). However, we know that the anharmonicity of the cavity field induced by the radiation pressure is not very large because the optomechanical interaction is usually not very strong. Therefore, the fidelity of the prepared target phonon state will be affected by the upper levels of the cavity field. To study how the small anharmonicity of the cavity field affects the fidelity of prepared nonclassical phonon states, we now study, as an example, the interaction between the mechanical resonator and three-level photon system, formed by three lowest energy levels  $|0\rangle \equiv |g\rangle$ ,  $|1\rangle \equiv |e\rangle$  and  $|2\rangle \equiv |e'\rangle$  of the cavity field. The transition frequency between the states  $|e\rangle$  and  $|e'\rangle$  is assumed as  $\omega + \delta$ . The parameter  $\delta$  characterizes the anharmonicity of the energy levels of the cavity field. The harmonic and the two-level model can be recovered when  $\delta = 0$  and  $\delta = \infty$ , respectively. In optomechanical systems, the anharmonicity is  $\delta = -2g^2/\omega_m$ , which is a negative number, i.e., the transition frequency between the states  $|e\rangle$  and  $|e'\rangle$  is smaller than that between the states  $|g\rangle$  and  $|e\rangle$ . As schematically shown in Fig. 2, the Hamiltonian  $H_{\text{thr}}$  between the three-level photon system and the mechanical mode can be written as

$$H_{\text{thr}} = \hbar\omega_m b^\dagger b + \hbar\omega |e\rangle\langle e| + \hbar(2\omega + \delta) |e'\rangle\langle e'| + \hbar \left\{ \Omega(t) \left[ |e\rangle\langle g| + \sqrt{2} |e'\rangle\langle e| \right] e^{\eta(b^\dagger - b)} + \text{h.c.} \right\}, \quad (27)$$

by projecting the cavity field operators  $a^\dagger$  and  $a$  in Eq. (2) to three eigenstates  $|g\rangle$ ,  $|e\rangle$  and  $|e'\rangle$  of the cavity field. Here, the parameter  $\Omega(t)$  in Eq. (27) is the same as that in Eq. (3).

If the ratio  $\eta$  is big enough, an arbitrary phonon state can be prepared by several red-sideband excitations after a carrier process, then the information leakage only occurs in the carrier process. In the carrier process for the time interval  $t_0^c = \pi/(2\Omega_{0,0})$ , the cavity field is prepared to its first excited state  $|e\rangle$  from the ground state  $|g\rangle$  under the two-level approximation in Eq. (3). However, when the information leakage from the first to the second excited state is considered, the wavefunction of the cavity field at the time  $t$  should be written as

$$|\varphi(t)\rangle = c_g(t)|g\rangle + c_e(t)|e\rangle + c_{e'}(t)|e'\rangle. \quad (28)$$

Three coefficients  $c_g(t)$ ,  $c_e(t)$ , and  $c_{e'}(t)$  can be obtained by solving the Schrodinger equation with given initial state  $|g\rangle$ . Thus, under the condition  $\Omega \ll |\delta|$ , the fidelity of preparing the excited state  $|e\rangle$  can be approximately given as

$$F = |\langle\varphi(t_0^c)|e\rangle|^2 \approx \left| \left(1 - \frac{3\Omega^2}{2\delta^2}\right) \sin \left[ \frac{\pi}{2} \left(1 - \frac{\Omega^2}{2\delta^2}\right) \right] \right|^2. \quad (29)$$

This type of information leakage has been studied in superconducting phase qubit systems [41].

If the ratio  $\eta$  is very small, then we need several carrier processes to generate the arbitrary superpositions of different phonon states. Thus, the fidelity calculation becomes complicated when the information leakage is included. Below, we discuss the information leakage in the limit  $\eta \ll 1$ . After we neglect the terms of  $O(\eta^2)$ , the Hamiltonian in Eq. (27) becomes

$$\begin{aligned} \tilde{H}_{\text{thr}} = & \hbar\omega_m b^\dagger b + \hbar\omega|e\rangle\langle e| + \hbar(2\omega + \delta)|e'\rangle\langle e'| \\ & + \hbar \left\{ \Omega(t) \left[ |e\rangle\langle g| + \sqrt{2}|e'\rangle\langle e| \right] [1 + \eta b^\dagger - \eta b] + \text{h.c.} \right\}. \end{aligned} \quad (30)$$

As an example, we analyze the effect of the third level  $|e'\rangle$  of the cavity field on the fidelities for preparing the phonon states  $|2\rangle$  and  $(|0\rangle - |2\rangle)/\sqrt{2}$  from the initial state  $|0, g\rangle$  by using the carrier and the single-phonon red sideband excitation processes. Let us first calculate the fidelity for preparing the state  $|2\rangle$  with the following steps:

$$\begin{array}{l} |0, g\rangle \xrightarrow{\text{(i) carrier}} |0, e\rangle \xrightarrow{\text{(ii) red sideband excitation}} |1, g\rangle \\ \xrightarrow{\text{(iii) carrier}} |1, e\rangle \xrightarrow{\text{(iv) red sideband excitation}} |2, g\rangle. \end{array}$$

At the initial time  $t_0$ , we have  $c_{0,g}(t_0) = 1$ , and the other coefficients are equal to zero. In the step (i), the system is excited to the state  $|0, e\rangle$  from the state  $|0, g\rangle$  by the external field with the carrier process, there is information leakage to the state  $|0, e'\rangle$  with a probability  $|c_{0,e'}(t_1^c)|^2$  in this process. For the time interval  $t_1^c = \pi/(2\Omega)$ , when the cavity field is prepared to the first excited state  $|e\rangle$  for the two-level approximation, the coefficient  $\tilde{c}_{0,e}(t_1)$ , that the system is in the state  $|0, e\rangle$  at the time  $t_1 = t_0 + t_1^c$ , can be given via Eq. (B11) in the Appendix B as

$$\tilde{c}_{0,e}(t_1) \approx -if_{ce} \quad (31)$$

when the third level of the cavity field is included, where

$$f_{ce} = \left(1 - \frac{3\Omega^2}{2\delta^2}\right) \sin \left[ \frac{\pi}{2} \left(1 - \frac{\Omega^2}{2\delta^2}\right) \right]. \quad (32)$$

In the step (ii), the system evolves to the state  $|1, g\rangle$  from the state  $|0, e\rangle$  via the red-sideband excitation process and there is no information leakage in this step. From Eq. (B16) in the Appendix B with the time interval  $t_2^r = \pi/(2\Omega\eta)$ , the coefficient  $\tilde{c}_{1,g}(t_2)$ , that the system is in the state  $|1, g\rangle$  at the time  $t_2 = t_1 + t_2^r$ , can be approximately given as

$$\tilde{c}_{1,g}(t_2) \approx i\tilde{c}_{0,e}(t_1). \quad (33)$$

In the step (iii), the system is prepared to the state  $|1, e\rangle$  from the state  $|1, g\rangle$  via the second carrier process with the information leakage to the state  $|1, e'\rangle$ . With the time interval  $t_3^c = \pi/(2\Omega)$ , the coefficient  $\tilde{c}_{1,e}(t_3)$ , that the system is in the state  $|1, e\rangle$  at the time  $t_3 = t_2 + t_3^c$ , can be obtained via Eq. (B11) in the Appendix B as

$$\tilde{c}_{1,e}(t_3) \approx -if_{ce}\tilde{c}_{1,g}(t_2). \quad (34)$$

In the step (iv), the system evolves to the state  $|2, g\rangle$  via the second red sideband excitation with the time interval  $t_4^r = \pi/(2\sqrt{2}\eta\Omega)$ , there is information leakage to the state  $|0, e'\rangle$  in this step. Using Eq. (B14) in the Appendix B, the coefficient  $\tilde{c}_{2,g}(t_4)$ , that the system is in the state  $|2, g\rangle$  at the time  $t_4 = t_3 + t_4^r$ , can be given as

$$\tilde{c}_{2,g}(t_4) \approx if_{rg}\tilde{c}_{1,e}(t_3). \quad (35)$$

where

$$f_{rg} = \left(1 - \frac{2(\eta\Omega)^2}{\delta^2}\right) \sin \left[ \frac{\pi}{2} \left(1 - \frac{3(\eta\Omega)^2}{4\delta^2}\right) \right]. \quad (36)$$

Because the fidelity to prepare the state  $|2\rangle$  is defined as

$$F_1 = |\langle 2, g | \varphi(t_4) \rangle|^2. \quad (37)$$

which can be given as

$$F_1 = |\tilde{c}_{2,g}(t_4)|^2. \quad (38)$$

From Eq. (31) to Eq. (36), we can approximately obtain

$$F_1 \approx |f_{rg}(f_{ce})^2|^2. \quad (39)$$

Similarly, the preparation of the state  $(|0\rangle - |2\rangle)/\sqrt{2}$  also needs four steps as for that of the state  $|2\rangle$ , but with different time intervals. Thus by using similar calculation steps, the fidelity  $F_2$ , for preparing the superposition  $(|0\rangle - |2\rangle)/\sqrt{2}$ , can be given as

$$F_2 \approx \frac{1}{4} |f_{cg}f_{ce} + f_{rg}(f_{ce})^2|^2. \quad (40)$$

Here, the parameters  $f_{ce}$  and  $f_{rg}$  are referred to Eqs. (32) and (36), however the parameter  $f_{cg}$  is given as

$$f_{cg} = \left(1 - \frac{2\Omega^2}{\delta^2}\right) \sin \left[ \frac{\pi}{2} \left(1 - \frac{\Omega^2}{2\delta^2}\right) \right]. \quad (41)$$

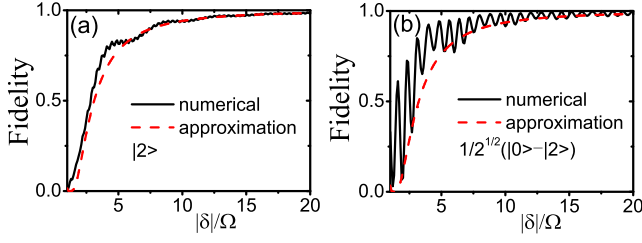


FIG. 3: (Color online) Fidelities are plotted as a function of  $|\delta|/\Omega$  for preparing states  $|2\rangle$  in (a) and  $(|0\rangle - |2\rangle)/\sqrt{2}$  in (b) using both numerical (black solid curve) and approximately analytical (red dash curve) results for  $\eta = 0.1$ .

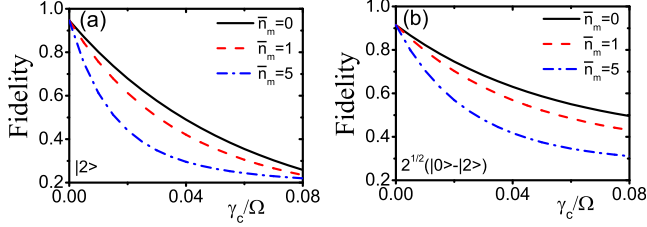


FIG. 4: (Color online) Fidelities are plotted for preparing states  $|2\rangle$  in (a) and  $(|0\rangle - |2\rangle)/\sqrt{2}$  in (b) as a function of the cavity decay rate  $\gamma_c/\Omega$  with different temperatures ( $\bar{n}_m = 0, 1, 5$ ) for  $\gamma_m = \gamma_c/10$ ,  $|\delta|/\Omega = 10$ , and  $\eta = 0.1$ .

In Figs. 3(a) and (b),  $F_1$  and  $F_2$  are numerically calculated and also compared with the approximated solutions in Eqs. (39) and (40). We find that the fidelities tend to one when  $|\delta|/\Omega > 20$ , moreover, the fidelity is bigger than 0.9 when  $|\delta|/\Omega > 10$ . Thus, it is clear that the large anharmonicity  $\delta$  corresponds to good two-level approximation.

## V. ENVIRONMENTAL EFFECT ON PHONON STATES PREPARATION

We now study the environmental effect on the phonon state preparation. After the environmental effect is included, the dynamical evolution of the reduced density operator  $\rho(t)$  of the optomechanical system can be described by using the master equation [48]

$$\begin{aligned} \frac{d\rho}{dt} = & \frac{1}{i\hbar} [H_{\text{eff}}, \rho] + \frac{\gamma_c}{2} (2\tilde{a}\rho\tilde{a}^\dagger - \tilde{a}^\dagger\tilde{a}\rho - \rho\tilde{a}^\dagger\tilde{a}) \\ & + \frac{\gamma_m}{2} (2\tilde{b}\rho\tilde{b}^\dagger - \tilde{b}^\dagger\tilde{b}\rho - \rho\tilde{b}^\dagger\tilde{b}) \\ & + \gamma_m\bar{n}_m (\tilde{b}\rho\tilde{b}^\dagger + \tilde{b}^\dagger\rho\tilde{b} - \tilde{b}^\dagger\tilde{b}\rho - \rho\tilde{b}\tilde{b}^\dagger), \end{aligned} \quad (42)$$

here,  $\gamma_m$  is the decay rate of mechanical mode and  $\bar{n}_m = 1/[\exp(\hbar\omega/k_B T) - 1]$  is the thermal phonon number of the mechanical resonator with the Boltzmann constant  $k_B$  and the environmental temperature  $T$ . In Eq. (42), we have set

$$\tilde{a} = UaU^\dagger = ae^{-\eta(b^\dagger - b)} \quad (43)$$

and

$$\tilde{b} = UbU^\dagger = b - \eta a^\dagger a. \quad (44)$$

When Eq. (42) is written out, we have assumed that the single-photon energy of the cavity field is much bigger than the thermal excitation energy and the single-phonon energy of the mechanical resonator, i.e.,  $\hbar\omega_c \gg k_B T$  and  $\hbar\omega_c \gg \hbar\omega_m$ , thus the thermal excitation on the cavity field is neglected under the condition of the low environmental temperature. In this case, the environment of the cavity field is assumed at the zero temperature, but the environmental temperature of the mechanical resonator is assumed as a finite value  $T$ .

In the limit  $\eta \ll 1$  and also for simplicity of the calculations, we can neglect the terms including, e.g.  $\eta\gamma_m b\rho a^\dagger a$  and  $O(\eta^2)$ , thus Eq. (42) is simplified to

$$\begin{aligned} \frac{d\rho}{dt} \approx & \frac{1}{i\hbar} [\tilde{H}_{\text{thr}}, \rho] + \frac{\gamma_c}{2} (2a\rho a^\dagger - a^\dagger a\rho - \rho a^\dagger a) \\ & + \frac{\gamma_m}{2} (2b\rho b^\dagger - b^\dagger b\rho - \rho b^\dagger b) \\ & + \gamma_m\bar{n}_m (b\rho b^\dagger + b^\dagger \rho b - b^\dagger b\rho - \rho b b^\dagger), \end{aligned} \quad (45)$$

with the photon operator given by

$$a \approx |g\rangle\langle e| + \sqrt{2}|e\rangle\langle e'|} \quad (46)$$

in the basis of three lowest energy levels of the photon system. The fidelity of the prepared phonon states can be calculated by [49]

$$F = \left[ \text{Tr} \left( \sqrt{\sqrt{\rho_r}\rho_t\sqrt{\rho_r}} \right) \right]^2, \quad (47)$$

where  $\rho_t$  is the density operator of the target phonon state and  $\rho_r$  is the reduced density operator of the mechanical resonator obtained by numerically solving the master equation (45).

The fidelities, for preparing states  $|2\rangle$  and  $(|0\rangle - |2\rangle)/\sqrt{2}$ , as a function of the cavity decay rate  $\gamma_c/\Omega$  are shown in Fig. 4. We find that the fidelities decrease with the increase of the decay rates of the cavity field and mechanical mode. To obtain the acceptable fidelity of the prepared state, the decay rates should be much smaller than the Rabi frequency of the external driven field, i.e.  $\gamma_c \ll \Omega$ . Moreover, the fidelities of the target states decrease with the increase of the thermal phonon in the mechanical resonator.

## VI. DISCUSSIONS ON EXPERIMENTAL FEASIBILITY

Let us now discuss the experimental feasibility of our proposal. (i) Similar to the ground-state cooling of the optomechanical system, the generation of arbitrary superpositions of phonon states relies on the sideband excitations. This means that the frequency  $\omega_m$  of the mechanical resonator and the decay rate  $\gamma_c$  of the cavity field have to satisfy the condition  $\omega_m > \gamma_c$ . (ii) Our proposal should work at the single-photon strong coupling regime as for the photon blockade [20, 21] in optomechanical systems, thus the coupling strength

TABLE I: Summary of the Lamb-Dicke parameters for current optomechanical experiments in microwave and optical domains. In the table,  $\omega_c$  and  $\gamma_c$  are the frequency and the decay rate of the cavity, the parameters  $\omega_m$  and  $\gamma_m$  are the frequency and the decay rate of the mechanical resonator,  $g$  is the optomechanical coupling constant, and  $\eta = g/\omega_m$  is the Lamb-Dicke parameter. The values given in parentheses are the expected experimental parameters achieved in the future for realizing our proposal.  $F_1$  and  $F_2$  are the fidelities for preparing states  $|2\rangle$  and  $(|0\rangle - |2\rangle)/\sqrt{2}$ , respectively. They are calculated at the zero temperature ( $\bar{n}_m = 0$ ) by using the parameters given in the parentheses with the corresponding Rabi frequency  $\Omega$ .

System	$\omega_c/2\pi$ (Hz)	$\gamma_c/2\pi$ (Hz)	$\omega_m/2\pi$ (Hz)	$\gamma_m/2\pi$ (Hz)	$g/2\pi$ (Hz)	$\eta = g/\omega_m$	$\Omega/2\pi$ (Hz)	$F_1$	$F_2$
Microwave cavity [17]	7.47 G	170 K (1 K)	10.69 M (100 M)	30 (10)	226 (10 M)	$2.11 \times 10^{-5}$ (0.1)	50 K	0.7359	0.8170
Toroidal microcavity [42]	385 T	7.1 M	78 M	10 K	3.4 K	$4.36 \times 10^{-5}$	-	-	-
Optomechanical crystals [31]	195 T	500 M (0.1 M)	3.68 G (10 G)	35 K (5 K)	910 K (1 G)	$2.47 \times 10^{-4}$ (0.1)	5 M	0.7205	0.8108
BEC [43]	385 T	1.3 M (0.1 M)	15.1 K (10 M)	(10)	0.39 M (1 M)	25.828 (0.1)	5 K	0.7017	0.8032
Membrane [44]	282 T	0.32 M	134 K	0.12	2.68	$2 \times 10^{-5}$	-	-	-
F-P cavity [45]	282 T	215 K	947 K	140	2.7	$2.85 \times 10^{-6}$	-	-	-
Zipper cavity [46]	194 T	6 G	7.9 M	98.75 K	599 K	$7.58 \times 10^{-2}$	-	-	-
Double-wheel microcavity [47]	190 T	10 G	8.05 M	2.01 M	732 K	$9.09 \times 10^{-2}$	-	-	-

$g$  and the frequency  $\omega_m$  of the mechanical resonator should be larger than the decay rates  $\gamma_c$  and  $\gamma_m$  of the mechanical resonator and the cavity field, i.e.,  $\omega_m, g \gg \gamma_c, \gamma_m$ . Moreover, the nonlinear photon-photon interaction strength  $g^2/\omega_m$  should be bigger than the decay rate  $\gamma_c$  of the cavity field, i.e.,  $(g^2/\omega_m) > \gamma_c$ , such that the single-photon excitation or photon blockade can be guaranteed and the two-level approximation can be applied. (iii) Negligible information leakage requires that the strength  $\Omega$  of the classical driving field should be smaller than the anharmonicity  $2g^2/\omega_m$  in the carrier pro-

cess. However, coherent transfer of excitations requires that the excitation time  $2\pi/\Omega$  of the cavity field should be much smaller than the decay times  $2\pi/\gamma_c$  of the cavity field for negligible temperature effect and  $2\pi/[(\bar{n}_m + 1)\gamma_m]$  of the mechanical mode at the finite temperature. Here, the thermal phonon number  $\bar{n}_m$  is referred to Eq. (42). (iv) As in trapped ion systems [9], the big Lamb-Dicke parameter  $\eta = g/\omega_m$  corresponds to the fast preparation of the multi-phonon states. Therefore, the big  $\eta$  is more desirable for our proposal.

Based on above discussions, we estimate experimental parameters for our goal. In Table I, we have summarized the parameters used for current experiments of optomechanical systems. We find that the promising candidates for realizing our proposal might be the optomechanical crystal devices [31], the ultracold atoms in optical resonators [15, 16] and superconducting circuits [17]. However, the parameters, e.g., the coupling strength  $g$  and the frequency  $\omega_m$  of the mechanical resonator, used for current experiments [15–17, 31] still need to be improved several orders of magnitude for our proposal. The improvements for decay rates  $\gamma_c$  and  $\gamma_m$  might be achieved by further increasing the quality factors of the optical cavity and mechanical resonator. However, the coupling constant  $g$  might be effectively increased by adding some impurities in the optomechanical systems [50]. In the zero temperature with  $\bar{n}_m = 0$ , we calculated the optimal fidelities  $F_1$  and  $F_2$  for the target states  $|2\rangle$  and  $(|0\rangle - |2\rangle)/\sqrt{2}$  using further possible parameters, as shown in parentheses of Table I, we find that the fidelities  $F_1 > 0.7$  and  $F_2 > 0.8$  can be achieved with these parameters.

## VII. CONCLUSIONS

In summary, we have proposed a method to synthesize arbitrary non-classical single-mode phonon states in optomechanical systems by combining photon blockade and sideband ex-

citations. Similar to the photon blockade [20, 21], our proposal relies on the single-photon strong coupling condition such that the two-level approximation for the cavity field can be made in the optomechanical systems. Our proposal opens up a possible way to deterministically engineer arbitrary non-classical single-mode phonon states on chip, and can also be generalized to engineering of multi-mode entangled phonon states in optomechanical systems [51]. The parameters, taken for calculations of the fidelities by us, are ambitious, but we hope that our proposal can be realized in the near future with significant improvement of the experiments.

## VIII. ACKNOWLEDGEMENT

Y.X.L. is supported by the National Natural Science Foundation of China under Nos. 10975080 and 61025022. J.Z. is supported by the NSFC under Nos. 61174084, 61134008.

## Appendix A: The time evolution operators

To show how the time evolution operators of the carrier, red and blue sideband precesses can be derived, it is convenient to work in the interaction picture by using

$$V = e^{iH_0t/\hbar} H_{\text{th}} e^{-iH_0t/\hbar} \quad (\text{A1})$$

with

$$H_0 = \hbar\omega_m b^\dagger b + (\hbar\omega\sigma_z)/2,$$

here, the Hamiltonian  $H_{\text{th}}$  is given in Eq. (4). Equation (A1) can be further expressed as

$$V = \hbar\Omega\sigma_+ e^{(-\frac{1}{2}\eta^2 - i\phi_d)} \sum_{j,j'} \frac{(-1)^{j'} \eta^{(j+j')}}{j!j'!} b^\dagger{}^j b^{j'} e^{-i\Delta t} + \text{h.c.}, \quad (\text{A2})$$

where  $\Delta = \omega_d - \omega + (j' - j)\omega_m$ . Using the Schrödinger equation, the wave function at any time  $t$  can be given by

$$|\psi(t)\rangle = U(t)|\psi(0)\rangle, \quad (\text{A3})$$

where  $U(t) = \exp(-iVt/\hbar)$  is the time evolution operator. By using the identity operator

$$\sum_{n=0}^{+\infty} \sum_{i=g,e} |n,i\rangle \langle i,n| = 1, \quad (\text{A4})$$

we can write out the time evolution operator  $U(t)$  explicitly for different resonant conditions. If the cavity is driven by a red-sideband excitation with the frequency of the driving field  $\omega_d = \omega - k\omega_m$ , then the time evolution operator is  $U_k^r(t^r) = \sum_{n=0}^{+\infty} U_{n,k}^r(t^r)$  for the time interval  $t^r$ , where  $U_{n,k}^r(t^r)$  is given by

$$U_{n,k}^r(t^r) = \begin{cases} |n,g\rangle \langle n,g| + [\cos(\Omega_{n,k}t^r)|n,e\rangle - i(-1)^k e^{i\phi_r} \sin(\Omega_{n,k}t^r)|n+k,g\rangle] \langle n,e| & n < k, \\ [\cos(\Omega_{n-k,k}t^r)|n,g\rangle - i(-1)^k e^{-i\phi_r} \sin(\Omega_{n-k,k}t^r)|n-k,e\rangle] \langle n,g| & n \geq k, \\ + [\cos(\Omega_{n,k}t^r)|n,e\rangle - i(-1)^k e^{i\phi_r} \sin(\Omega_{n,k}t^r)|n+k,g\rangle] \langle n,e| & \end{cases} \quad (\text{A5})$$

with the Rabi frequency

$$\Omega_{n,k} = \Omega\eta^k e^{-\frac{1}{2}\eta^2} \sqrt{\frac{(n+k)!}{n!}} \sum_{j=0}^n \frac{(-1)^j \eta^{2j}}{j!(j+k)!(n-j)!}. \quad (\text{A6})$$

When the cavity is driven by blue-sideband excitation with the frequency  $\omega_d = \omega + k\omega_m$ , then the time evolution operator is  $U_k^b(t^b) = \sum_{n=0}^{+\infty} U_{n,k}^b(t^b)$  with the time interval  $t^b$ , where  $U_{n,k}^b(t^b)$  is given as

$$U_{n,k}^b(t^b) = \begin{cases} [\cos(\Omega_{n,k}t^b)|n,g\rangle - ie^{-i\phi_b} \sin(\Omega_{n,k}t^b)|n+k,e\rangle] \langle n,g| + |n,e\rangle \langle n,e| & n < k, \\ [\cos(\Omega_{n,k}t^b)|n,g\rangle - ie^{-i\phi_b} \sin(\Omega_{n,k}t^b)|n+k,e\rangle] \langle n,g| & n \geq k. \\ + [\cos(\Omega_{n-k,k}t^b)|n,e\rangle - ie^{i\phi_b} \sin(\Omega_{n-k,k}t^b)|n-k,g\rangle] \langle n,e| & \end{cases} \quad (\text{A7})$$

Finally, if the driving field is resonant with the two-lowest energy levels of the cavity field, e.g.  $\omega_d = \omega$ , then the carrier process occurs and the time evolution operator is  $U^c(t^c) = \sum_{n=0}^{+\infty} U_{n,0}^c(t^c)$  with the time interval  $t^c$ , where  $U_{n,0}^c(t^c)$  is given by

$$U_{n,0}^c(t^c) = [\cos(\Omega_{n,0}t^c)|n,g\rangle - ie^{-i\phi_c} \sin(\Omega_{n,0}t^c)|n,e\rangle] \langle n,g| + [\cos(\Omega_{n,0}t^c)|n,e\rangle - ie^{i\phi_c} \sin(\Omega_{n,0}t^c)|n,g\rangle] \langle n,e|. \quad (\text{A8})$$

Under different resonant conditions, dynamical evolutions of the system are governed by the red sideband excitation, blue sideband excitation, and carrier process with the time evolution operators given in Eqs. (A5)-(A8), respectively.

### Appendix B: Leakage effect

In order to analyze the effect of the third level  $|e'\rangle$  of the cavity field on the fidelity for preparing the phonon states  $|2\rangle$  and  $(|0\rangle - |2\rangle)/\sqrt{2}$  from the initial state  $|0,g\rangle$ , let us assume that the wavefunction of the optomechanical system for the

carrier and sideband excitations can be written as

$$|\varphi(t)\rangle = c_{0,g}(t)|0,g\rangle + c_{1,g}(t)|1,g\rangle + c_{2,g}(t)|2,g\rangle + c_{0,e}(t)|0,e\rangle + c_{1,e}(t)|1,e\rangle + c_{2,e}(t)|2,e\rangle + c_{0,e'}(t)|0,e'\rangle + c_{1,e'}(t)|1,e'\rangle + c_{2,e'}(t)|2,e'\rangle, \quad (\text{B1})$$

at the time  $t$ , where sideband excitation includes only the single-phonon process.

For the carrier process,  $\omega_d = \omega$  and there is no phonon exchange when the photon is excited, thus there is no transition between phonon Fock states with different phonon numbers and the coefficients  $c_{m,i}(t)$  in Eq. (B1) satisfy the dynamical

equations

$$i\partial_t \begin{pmatrix} \tilde{c}_{0,g} \\ \tilde{c}_{0,e} \\ \tilde{c}_{0,e'} \\ \tilde{c}_{1,g} \\ \tilde{c}_{1,e} \\ \tilde{c}_{1,e'} \\ \tilde{c}_{2,g} \\ \tilde{c}_{2,e} \\ \tilde{c}_{2,e'} \end{pmatrix} = \begin{pmatrix} 0 & \Omega & 0 & 0 & 0 & 0 & 0 & 0 & 0 \\ \Omega & 0 & \sqrt{2}\Omega & 0 & 0 & 0 & 0 & 0 & 0 \\ 0 & \sqrt{2}\Omega & \delta & 0 & 0 & 0 & 0 & 0 & 0 \\ \hline 0 & 0 & 0 & 0 & \Omega & 0 & 0 & 0 & 0 \\ 0 & 0 & 0 & \Omega & 0 & \sqrt{2}\Omega & 0 & 0 & 0 \\ 0 & 0 & 0 & 0 & \sqrt{2}\Omega & \delta & 0 & 0 & 0 \\ \hline 0 & 0 & 0 & 0 & 0 & 0 & 0 & \Omega & 0 \\ 0 & 0 & 0 & 0 & 0 & 0 & \Omega & 0 & \sqrt{2}\Omega \\ 0 & 0 & 0 & 0 & 0 & 0 & 0 & \sqrt{2}\Omega & \delta \end{pmatrix} \begin{pmatrix} \tilde{c}_{0,g} \\ \tilde{c}_{0,e} \\ \tilde{c}_{0,e'} \\ \tilde{c}_{1,g} \\ \tilde{c}_{1,e} \\ \tilde{c}_{1,e'} \\ \tilde{c}_{2,g} \\ \tilde{c}_{2,e} \\ \tilde{c}_{2,e'} \end{pmatrix}, \quad (\text{B2})$$

where  $m = 0, 1, 2$  denote the phonon states and  $i = g, e, e'$  denote the photon states. In Eq. (B2), we have also used the relations

$$\begin{aligned} \tilde{c}_{m,g} &= c_{m,g} \exp(im\omega_m t), \\ \tilde{c}_{m,e} &= c_{m,e} \exp[i(\omega_d + m\omega_m) t], \\ \tilde{c}_{m,e'} &= c_{m,e'} \exp[i(2\omega_d + m\omega_m) t]. \end{aligned} \quad (\text{B3})$$

For the red sideband excitation with  $\omega_d = \omega - \omega_m$ , we can also have

$$i\partial_t \begin{pmatrix} \tilde{c}_{0,g} \\ \tilde{c}_{1,g} \\ \tilde{c}_{0,e} \\ \tilde{c}_{2,g} \\ \tilde{c}_{1,e} \\ \tilde{c}_{0,e'} \\ \tilde{c}_{2,e} \\ \tilde{c}_{1,e'} \\ \tilde{c}_{2,e'} \end{pmatrix} = \begin{pmatrix} 0 & 0 & 0 & 0 & 0 & 0 & 0 & 0 & 0 \\ 0 & 0 & -\eta\Omega & 0 & 0 & 0 & 0 & 0 & 0 \\ 0 & -\eta\Omega & 0 & 0 & 0 & 0 & 0 & 0 & 0 \\ \hline 0 & 0 & 0 & 0 & -\eta\Omega\sqrt{2} & 0 & 0 & 0 & 0 \\ 0 & 0 & 0 & -\eta\Omega\sqrt{2} & 0 & -\eta\Omega\sqrt{2} & 0 & 0 & 0 \\ 0 & 0 & 0 & 0 & -\eta\Omega\sqrt{2} & \delta & 0 & 0 & 0 \\ \hline 0 & 0 & 0 & 0 & 0 & 0 & 0 & -2\eta\Omega & 0 \\ 0 & 0 & 0 & 0 & 0 & 0 & -2\eta\Omega & \delta & 0 \\ 0 & 0 & 0 & 0 & 0 & 0 & 0 & 0 & \delta \end{pmatrix} \begin{pmatrix} \tilde{c}_{0,g} \\ \tilde{c}_{1,g} \\ \tilde{c}_{0,e} \\ \tilde{c}_{2,g} \\ \tilde{c}_{1,e} \\ \tilde{c}_{0,e'} \\ \tilde{c}_{2,e} \\ \tilde{c}_{1,e'} \\ \tilde{c}_{2,e'} \end{pmatrix}. \quad (\text{B4})$$

The dynamical evolutions of the system in different conditions can be obtained by numerically solving Eqs. (B2) and (B4). However, we can approximately give an analytical solution by using the method in Ref. [41] as shown below.

The left matrixes of the right hand of the dynamical equations in Eqs. (B2) and (B4) have block diagonal form, thus the calculations on total solutions of Eqs. (B2) and (B4) can be greatly reduced. It is clear that the problem of solving Eq. (B2) is equivalent to that of solving three linear differential equations

$$\begin{aligned} i\partial_t \tilde{c}_G &= A\tilde{c}_E, \\ i\partial_t \tilde{c}_E &= A\tilde{c}_G + B\tilde{c}_{E'}, \\ i\partial_t \tilde{c}_{E'} &= B\tilde{c}_E + \delta\tilde{c}_{E'}, \end{aligned} \quad (\text{B5})$$

where  $A = \Omega$ ,  $B = \sqrt{2}\Omega$ , the subscript  $G(= m, g)$  denotes that the cavity field is in the ground state with  $m$  phonons. The subscript  $E(= m, e)$  or  $E'(= m, e')$  denote that the cavity field is in the first or the second excited state with  $m$  phonons.

Here,  $m$  takes values 0, 1 and 2, which correspond to three different block matrixes.

In the condition  $\delta \gg |A|, |B|$ , the general solutions of Eq. (B5) can be given as

$$\begin{aligned} \tilde{c}_G(t) &= \sum_{n=1}^3 c_n \exp(-i\omega_n t), \\ \tilde{c}_E(t) &= \frac{1}{A} \sum_{n=1}^3 \omega_n c_n \exp(-i\omega_n t), \\ \tilde{c}_{E'}(t) &= \frac{1}{AB} \sum_{n=1}^3 (\omega_n^2 - A^2) c_n \exp(-i\omega_n t), \end{aligned} \quad (\text{B6})$$

with

$$\begin{aligned}\omega_1 &= \frac{\Omega_R}{2} - \frac{B^2}{2\delta}, \\ \omega_2 &= -\frac{\Omega_R}{2} - \frac{B^2}{2\delta}, \\ \omega_3 &= \delta \left(1 + \frac{B^2}{\delta^2}\right),\end{aligned}\quad (\text{B7})$$

with the parameter  $\Omega_R$ , defined as

$$\Omega_R = 2|A| \left(1 - \frac{B^2}{2\delta^2} + \frac{B^4}{8A^2\delta^2}\right). \quad (\text{B8})$$

The coefficients  $c_n$  in Eq. (B6) with  $n = 1, 2, 3$  can be determined by the initial condition.

If the cavity field and the mechanical mode are initially in the ground state  $|g\rangle$  and  $m$ -phonon state  $|m\rangle$ , respectively, i.e., the initial state of the system is  $|m, g\rangle$ , then we have  $\tilde{c}_G(0) = 1$ ,  $\tilde{c}_E(0) = \tilde{c}_{E'}(0) = 0$ , and thus the coefficients  $c_n$  satisfy following linear equations

$$\begin{aligned}c_1 + c_2 + c_3 &= 1, \\ \omega_1 c_1 + \omega_2 c_2 + \omega_3 c_3 &= 0, \\ \omega_1^2 c_1 + \omega_2^2 c_2 + \omega_3^2 c_3 &= A^2.\end{aligned}\quad (\text{B9})$$

In the condition  $\delta \gg |A|, |B|$ , we obtain

$$\begin{aligned}c_1 &\approx \frac{1}{2} + \frac{B^2}{4|A|\delta}, \\ c_2 &\approx \frac{1}{2} - \frac{B^2}{4|A|\delta}, \\ c_3 &\approx 0.\end{aligned}\quad (\text{B10})$$

Thus, we have the solutions

$$\begin{aligned}\tilde{c}_G(t) &\approx \cos\left(\frac{\Omega_R t}{2}\right) - i\frac{B^2}{2|A|\delta} \sin\left(\frac{\Omega_R t}{2}\right), \\ \tilde{c}_E(t) &\approx -i\frac{|A|}{A} \left(1 - \frac{B^2}{2\delta^2} - \frac{B^4}{8A^2\delta^2}\right) \sin\left(\frac{\Omega_R t}{2}\right), \\ \tilde{c}_{E'}(t) &\approx i\frac{|A|}{A} \frac{B}{\delta} \sin\left(\frac{\Omega_R t}{2}\right),\end{aligned}\quad (\text{B11})$$

when the whole system is initially in the ground state. Similarly, if the system is initially in the state  $|m, e\rangle$ , i.e.,  $\tilde{c}_E(0) = 1$ ,  $\tilde{c}_G(0) = \tilde{c}_{E'}(0) = 0$ , then we have

$$\begin{aligned}c_1 + c_2 + c_3 &= 0, \\ \omega_1 c_1 + \omega_2 c_2 + \omega_3 c_3 &= A, \\ \omega_1^2 c_1 + \omega_2^2 c_2 + \omega_3^2 c_3 &= 0.\end{aligned}\quad (\text{B12})$$

By solving above linear equations in the condition  $\delta \gg |A|, |B|$ , we can have

$$\begin{aligned}c_1 &\approx \frac{A}{2|A|} \left(1 - \frac{B^2}{\delta^2}\right), \\ c_2 &\approx -\frac{A}{2|A|} \left(1 - \frac{B^2}{\delta^2}\right), \\ c_3 &\approx \frac{AB^2}{\delta^3}.\end{aligned}\quad (\text{B13})$$

Then, we have the solutions

$$\begin{aligned}\tilde{c}_G(t) &\approx -i\frac{A}{|A|} \left(1 - \frac{B^2}{\delta^2}\right) \sin\left(\frac{\Omega_R t}{2}\right), \\ \tilde{c}_E(t) &\approx \left(1 - \frac{3B^2}{2\delta^2} + \frac{B^4}{8A^2\delta^2}\right) \cos\left(\frac{\Omega_R t}{2}\right), \\ \tilde{c}_{E'}(t) &\approx \frac{B}{\delta} \left\{ \cos\left[\left(\delta + \frac{3B^2}{2\delta}\right)t\right] - \cos\left(\frac{\Omega_R t}{2}\right) \right\} \\ &\quad - i\frac{B}{\delta} \sin\left[\left(\delta + \frac{3B^2}{2\delta}\right)t\right],\end{aligned}\quad (\text{B14})$$

when the whole system is initially in the state  $|m, e\rangle$ .

Similarly, the solutions of Eq. (B4) can be given by solving the linear differential equations. The solutions of the coefficients  $\tilde{c}_{2,g}$ ,  $\tilde{c}_{1,e}$  and  $\tilde{c}_{0,e'}$  can be given by solving Eq. (B5) with  $A = B = -\eta\Omega\sqrt{2}$  and the subscripts are taken as  $G = (2, g)$ ,  $E = (1, e)$ , and  $E' = (0, e')$ . The coefficient  $\tilde{c}_{0,g}$  ( $\tilde{c}_{2,e'}$ ) only depends on itself and initial condition. The coefficients  $\tilde{c}_{1,g}$  and  $\tilde{c}_{0,e}$  ( $\tilde{c}_{2,e}$  and  $\tilde{c}_{1,e'}$ ) satisfy the following linear differential equations

$$\begin{aligned}i\partial_t \tilde{c}_S &= A' \tilde{c}_X, \\ i\partial_t \tilde{c}_X &= A' \tilde{c}_S + B' \tilde{c}_X,\end{aligned}\quad (\text{B15})$$

for  $A' = -\eta\Omega$  and  $B' = 0$  with the subscripts  $S = (1, g)$  and  $X = (0, e)$  [ $A' = -2\eta\Omega$ ,  $B' = \delta$  with the subscripts  $S = (2, e)$  and  $X = (1, e')$ ]. The general solutions of Eq. (B15) are given by

$$\begin{aligned}\tilde{c}_S(t) &= \left\{ \tilde{c}_S(0) \left[ \cos\left(\frac{\Omega_{R'}}{2}t\right) + \frac{iB'}{\Omega_{R'}} \sin\left(\frac{\Omega_{R'}}{2}t\right) \right] \right. \\ &\quad \left. - i\frac{2A'}{\Omega_{R'}} \tilde{c}_X(0) \sin\left(\frac{\Omega_{R'}}{2}t\right) \right\} e^{-iB't/2} \\ \tilde{c}_X(t) &= \left\{ \tilde{c}_X(0) \left[ \cos\left(\frac{\Omega_{R'}}{2}t\right) - \frac{iB'}{\Omega_{R'}} \sin\left(\frac{\Omega_{R'}}{2}t\right) \right] \right. \\ &\quad \left. - i\frac{2A'}{\Omega_{R'}} \tilde{c}_S(0) \sin\left(\frac{\Omega_{R'}}{2}t\right) \right\} e^{-iB't/2}\end{aligned}\quad (\text{B16})$$

where  $\Omega_{R'} = \sqrt{4A'^2 + B'^2}$ .

- 
- [1] M. Poot and H. S. J. van der Zant, Phys. Rep. **511**, 273 (2012).  
[2] T. J. Kippenberg and K. J. Vahala, Science **321**, 1172 (2008).  
[3] M. Aspelmeyer, S. Gröblacher, K. Hammerer, and N. Kiesel, J.

- Opt. Soc. Am. B **27**, A189 (2010).  
[4] Y. X. Liu, L. F. Wei, and F. Nori, Europhys. Lett. **67**, 941 (2004).

- [5] M. Hofheinz, E. M. Weig, M. Ansmann, R. C. Bialczak, E. Lucero, M. Neeley, A. D. O'Connell, H. Wang, J. M. Martinis, and A. N. Cleland, *Nature* **454**, 310 (2008).
- [6] M. Hofheinz, H. Wang, M. Ansmann, R. C. Bialczak, E. Lucero, M. Neeley, A. D. O'Connell, D. Sank, J. Wenner, J. M. Martinis, and A. N. Cleland, *Nature* **459**, 546 (2009).
- [7] S. A. Gardiner, J. I. Cirac, and P. Zoller, *Phys. Rev. A* **55**, 1683 (1997).
- [8] S. B. Zheng, *Phys. Rev. A* **63**, 015801 (2001).
- [9] L. F. Wei, Y. X. Liu, and F. Nori, *Phys. Rev. A* **70**, 063801 (2004).
- [10] D. Leibfried, R. Blatt, C. Monroe, and D. Wineland, *Rev. Mod. Phys.* **75**, 281 (2003).
- [11] D. M. Meekhof, C. Monroe, B. E. King, W. M. Itano, and D. J. Wineland, *Phys. Rev. Lett.* **76**, 1796 (1996).
- [12] D. Leibfried, D. M. Meekhof, B. E. King, C. Monroe, W. M. Itano, and D. J. Wineland, *Phys. Rev. Lett.* **77**, 4281 (1996).
- [13] A. D. Armour, M. P. Blencowe, and K. C. Schwab, *Phys. Rev. Lett.* **88**, 148301 (2002).
- [14] A. D. O'Connell, M. Hofheinz, M. Ansmann, R. C. Bialczak, M. Lenander, E. Lucero, M. Neeley, D. Sank, H. Wang, M. Weides, J. Wenner, J. M. Martinis, and A. N. Cleland, *Nature* **464**, 697 (2010).
- [15] S. Gupta, K. L. Moore, K. W. Murch, and D. M. Stamper-Kurn, *Phys. Rev. Lett.* **99**, 213601 (2007).
- [16] M. Eichenfield, J. Chan, R. M. Camacho, K. J. Vahala, and O. Painter, *Nature* **462**, 78 (2009).
- [17] J. D. Teufel, D. Li, M. S. Allman, K. Cicak, A. J. Sirois, J. D. Whittaker, and R. W. Simmonds, *Nature* **471**, 204 (2011).
- [18] J. C. Sankey, C. Yang, B. M. Zwickl, A. M. Jayich, and J. G. E. Harris, *Nature Phys.* **6**, 707 (2010).
- [19] A. Imamoglu, H. Schmidt, G. Woods, and M. Deutsch, *Phys. Rev. Lett.* **79**, 1467 (1997).
- [20] P. Rabl, *Phys. Rev. Lett.* **107**, 063601 (2011).
- [21] A. Nunnenkamp, K. Borkje, and S. M. Girvin, *Phys. Rev. Lett.* **107**, 063602 (2011).
- [22] B. He, *Phys. Rev. A* **85**, 063820 (2012).
- [23] J. Q. Liao, H. K. Cheung, and C. K. Law, *Phys. Rev. A* **85**, 025803 (2012).
- [24] J. Q. Liao and F. Nori, *Phys. Rev. A* **88**, 023853 (2013).
- [25] I. Wilson-Rae, N. Nooshi, W. Zwerger, and T. J. Kippenberg, *Phys. Rev. Lett.* **99**, 093901 (2007).
- [26] F. Marquardt, J. P. Chen, A. A. Clerk, and S. M. Girvin, *Phys. Rev. Lett.* **99**, 093902 (2007).
- [27] Y. S. Park and H. L. Wang, *Nature Phys.* **5**, 489 (2009).
- [28] A. Schliesser, R. Riviere, G. Anetsberger, O. Arcizet, and T. J. Kippenberg, *Nature Phys.* **4**, 415 (2008).
- [29] A. Schliesser, O. Arcizet, R. Riviere, G. Anetsberger, and T. J. Kippenberg, *Nature Phys.* **5**, 509 (2009).
- [30] J. D. Teufel, T. Donner, D. Li, J. W. Harlow, M. S. Allman, K. Cicak, A. J. Sirois, J. D. Whittaker, K. W. Lehnert, and R. W. Simmonds, *Nature* **475**, 359 (2011).
- [31] J. Chan, T. P. M. Alegre, A. H. Safavi-Naeini, J. T. Hill, A. Krause, S. Groblacher, M. Aspelmeyer, and O. Painter, *Nature* **478**, 89 (2011).
- [32] A. H. Safavi-Naeini, J. Chan, J. T. Hill, S. Gröblacher, H. Miao, Y. Chen, M. Aspelmeyer and O. Painter, *New J. Phys.* **15**, 035007 (2013).
- [33] W. Marshall, C. Simon, R. Penrose, and D. Bouwmeester, *Phys. Rev. Lett.* **91**, 130401 (2003).
- [34] B. Pepper, R. Ghobadi, E. Jeffrey, C. Simon, and D. Bouwmeester, *Phys. Rev. Lett.* **109**, 023601 (2012).
- [35] M. R. Vanner, M. Aspelmeyer, M. S. Kim, *Phys. Rev. Lett.* **110**, 010504 (2013).
- [36] F. Khalili, S. Danilishin, H. Miao, H. Müller-Ebhardt, H. Yang, and Y. Chen, *Phys. Rev. Lett.* **105**, 070403 (2010).
- [37] O. Romero-Isart, A. C. Pflanzer, F. Blaser, R. Kaltenbaek, N. Kiesel, M. Aspelmeyer, and J. I. Cirac, *Phys. Rev. Lett.* **107**, 020405 (2011).
- [38] C. A. Blockley, D. F. Walls, and H. Risken, *Europhys. Lett.* **17**, 509 (1992).
- [39] C. K. Law and J. H. Eberly, *Phys. Rev. Lett.* **76**, 1055 (1996).
- [40] B. Kneer and C. K. Law, *Phys. Rev. A* **57**, 2096 (1998).
- [41] M. H. S. Amin, *Low Temp. Phys.* **32**, 198 (2006).
- [42] E. Verhagen, S. Deleglise, S. Weis, A. Schliesser, and T. J. Kippenberg, *Nature* **482**, 63 (2012).
- [43] F. Brennecke, S. Ritter, T. Donner, and T. Esslinger, *Science* **322**, 235 (2008).
- [44] J. D. Thompson, B. M. Zwickl, A. M. Jayich, F. Marquardt, S. M. Girvin, and J. G. E. Harris, *Nature* **452**, 72 (2008).
- [45] S. Groblacher, K. Hammerer, M. R. Vanner, and M. Aspelmeyer, *Nature* **460**, 724 (2009).
- [46] M. Eichenfield, R. Camacho, J. Chan, K. J. Vahala, and O. Painter, *Nature* **459**, 550 (2009).
- [47] G. S. Wiederhecker, S. Manipatruni, S. Lee, and M. Lipson, *Opt. Exp.* **19**, 2782 (2011).
- [48] H. J. Carmichael, *An Open Systems Approach to Quantum Optics*, (Springer-Verlag, Berlin, 1993).
- [49] A. Uhlmann, *Rep. Math. Phys.* **9**, 273 (1976).
- [50] H. Ian, Z. R. Gong, Y. X. Liu, C. P. Sun, and F. Nori, *Phys. Rev. A* **78**, 013824 (2008).
- [51] X. W. Xu, Y. J. Zhao, and Y. X. Liu, *Phys. Rev. A* **88**, 022325 (2013).